

# $\mathcal{O}(\alpha_s)$ corrections to $J/\psi + \chi_{cJ}$ production at $B$ factories

Hai-Rong Dong<sup>\*,1</sup> Feng Feng<sup>†,2,1</sup> and Yu Jia<sup>‡3,1,2</sup>

<sup>1</sup>*Institute of High Energy Physics, Chinese Academy of Sciences, Beijing 100049, China*

<sup>2</sup>*Theoretical Physics Center for Science Facilities,  
Chinese Academy of Sciences, Beijing 100049, China*

<sup>3</sup>*Maryland Center for Fundamental Physics, Department of Physics,  
University of Maryland, College Park, MD 20742, USA*

(Dated: September 22, 2021)

## Abstract

We investigate the  $\mathcal{O}(\alpha_s)$  corrections to  $e^+e^- \rightarrow J/\psi(\psi') + \chi_{cJ}$  ( $J = 0, 1, 2$ ) in the NRQCD factorization approach. These next-to-leading order (NLO) corrections are calculated at the level of helicity amplitude. We have made a detailed analysis for both polarized and unpolarized cross sections, and compared our predictions with the measurements at the  $B$  factories. We also derive the asymptotic expressions for each of the NLO helicity amplitudes, and confirm the earlier speculation that at NLO in  $\alpha_s$ , the double logarithm of type  $\ln^2(s/m_c^2)$  appearing in the NRQCD short-distance coefficient is always associated with the helicity-suppressed channels.

PACS numbers: *12.38.Bx, 13.66.Bc, 13.88.+e, 14.40.Pq*

---

\* E-mail: donghr@ihep.ac.cn

† E-mail: fengf@ihep.ac.cn

‡ E-mail: jiay@ihep.ac.cn

## 1. INTRODUCTION

The studies of hard exclusive reactions have historically played an important role in the development of perturbative Quantum Chromodynamics (pQCD). The standard theoretical tool is the light-cone (collinear factorization) approach, which is based on the expansion in powers of  $1/Q$ , where  $Q^2$  characterizes the hard momentum transfer [1, 2]. The classic applications of light-cone factorization are exemplified by the  $\pi-\gamma$  transition form factor,  $\pi$  electromagnetic (EM) form factor [1, 2], and the  $B$  meson exclusive decays [3, 4], to which a vast amount of literature has been devoted.

Recent advancement of the high-luminosity high-energy collider facilities renders the study of hard exclusive processes involving heavy quarkonium a fertile new research frontier. Perhaps a great amount of interest toward this topic was triggered by the observation of several double-charmonium production processes in two  $B$  factories several years ago [5, 6].

In addition to the light-cone approach, there also exists another relatively new factorization approach, the *NRQCD factorization* [7], which is tailor-made to tackle quarkonium production and decay processes. Explicitly exploiting the nonrelativistic nature of quarkonium, the NRQCD factorization approach allows one to express the amplitude of an exclusive quarkonium production reaction in terms of an infinite sum of products of short-distance coefficients and the vacuum-to-quarkonium NRQCD matrix elements, whose importance is organized by the powers of  $v$ , the typical velocity of a heavy quark inside the quarkonium.

Perhaps the most famous example of double charmonium production is  $e^+e^- \rightarrow J/\psi + \eta_c$ , with the interest originally spurred by the alarming discrepancy between the BELLE measurement [5] and the leading-order (LO) NRQCD predictions [8–10]. In the following years, this process has been intensively studied in both of the NRQCD and light-cone frameworks [8–15].

One of the important steps toward alleviating the discrepancy between data and theory for  $e^+e^- \rightarrow J/\psi + \eta_c$  is the discovery of significant and positive NLO perturbative corrections [11, 12]. This NLO calculation was performed in NRQCD factorization. In contrast, due to some long-standing theoretical difficulty inherent to this helicity-suppressed process, by far no one has successfully worked out the NLO correction to this process in the light-cone approach.

Besides  $e^+e^- \rightarrow J/\psi + \eta_c$ , two  $B$  factories have also measured several other double-charmonium production processes [5, 6], notably  $e^+e^- \rightarrow J/\psi + \chi_{cJ}$  ( $J = 0, 1, 2$ ). Recently in Ref. [16], the NLO perturbative correction was performed for  $e^+e^- \rightarrow J/\psi + \chi_{c0}$  at LO in  $v$  and a rather large  $K$  factor was reported to bring the theory prediction in better agreement with the measurement. Nevertheless, at this stage, both  $B$  factory experiments have not clearly observed any  $J/\psi + \chi_{c1,2}$  events yet, even with latest data set [17], and only an upper bound for the production cross sections is placed.

The purpose of this work is to carry out a comprehensive next-to-leading order (NLO) perturbative analysis to  $e^+e^- \rightarrow J/\psi(\psi') + \chi_{cJ}$  ( $J = 0, 1, 2$ ) at the lowest order in  $v$ . We will work out the NLO corrections to each of the helicity amplitudes, so that we can address their impact on both the polarized and unpolarized cross sections.

We find a large positive NLO perturbative correction to  $e^+e^- \rightarrow J/\psi + \chi_{c0}$ , which is helpful to bring the predicted cross section closer to the  $B$  factory measurements. However, our NLO predictions to  $\psi' + \chi_{c0}$  cross section seems still significantly below the central value of the BELLE measurement.

On the other hand, the impact of NLO corrections to  $e^+e^- \rightarrow J/\psi + \chi_{c1,2}$  seems to be rather modest, even with their signs uncertain. Our predicted cross sections for these

processes are about 5 or 6 times smaller than that for  $e^+e^- \rightarrow J/\psi + \chi_{c0}$ . Hopefully the future Super  $B$  factory, with much higher luminosity, will eventually observe these two channels.

Our studies of polarized cross sections reveal that the bulk of the total cross section comes from the  $(0, \pm 1)$  helicity states for  $e^+e^- \rightarrow J/\psi + \chi_{c1}$ , and from the  $(0, 0)$  and  $(\pm 1, 0)$  helicity states for  $e^+e^- \rightarrow J/\psi + \chi_{c2}$ . It will be interesting for the future Super  $B$  experiments to test these polarization patterns.

From the theoretical perspective, we have also presented the analytic asymptotic expressions of all the ten NLO helicity amplitudes for the  $e^+e^- \rightarrow J/\psi + \chi_{cJ}$  ( $J = 0, 1, 2$ ) processes. The logarithmical scaling-violation pattern is recognized in these NLO asymptotic expressions, which supports for the speculation made in Ref. [18]: The hard exclusive processes involving double-quarkonium at leading twist can only host the single collinear logarithm  $\ln s/m_c^2$  at one-loop, while those beginning with the higher twist contributions are always plagued with double logarithms of form  $\ln^2 s/m_c^2$ . It would be theoretically interesting to reproduce these asymptotic expressions by using the light-cone approach.

The rest of the paper is organized as follows. In Section 2, we present a concise review on the helicity amplitude formalism and helicity selection rule, taking the process  $e^-e^+ \rightarrow J/\psi + \chi_{cJ}$  ( $J = 0, 1, 2$ ) as the example. In Section 3, we rederive the tree-level predictions in the NRQCD factorization approach, and present the LO expressions for all the involved helicity amplitudes. In Section 4, we first elaborate on some key technical issues about the NLO perturbative calculations, then present the asymptotic expressions for the NLO corrections for all the encountered helicity amplitudes. The pattern of the logarithmic scaling violation is recognized, and their implication with the light-cone approach is discussed. We devote Section 5 to explore the phenomenological impact of our NLO predictions on the  $B$  factory measurements. A comprehensive numerical study is performed for both unpolarized and polarized cross sections of the  $e^-e^+ \rightarrow J/\psi + \chi_{cJ}$  ( $J = 0, 1, 2$ ) processes. Finally, we summarize in Section 5.

## 2. POLARIZED CROSS SECTIONS AND HELICITY SELECTION RULE

It is often desirable to know the polarization information for an exclusive reaction, especially for the double-charmonium production process considered in this work. To fulfill this goal, one can employ the *helicity amplitude formalism* [19], which appears to be a quite convenient and advantageous tool both experimentally and theoretically.

Suppose the  $e^-$  and  $e^+$  beams are aligned along the  $\hat{z}$  direction, bearing the invariant mass of  $\sqrt{s}$ . We will choose to work in their center-of-mass frame. Let  $\theta$  denote the angle between the moving directions of  $J/\psi$  and  $e^-$ , and  $|\mathbf{P}|$  signify the magnitude of the momentum carried by the  $J/\psi$  ( $\chi_{cJ}$ ) [Note that  $|\mathbf{P}| = \lambda^{\frac{1}{2}}(s, M_{J/\psi}^2, M_{\chi_{cJ}}^2)/(2\sqrt{s})$ , where  $\lambda(x, y, z) = x^2 + y^2 + z^2 - 2xy - 2yz - 2zx$ ]. Assume the outgoing  $J/\psi$  and  $\chi_{cJ}$  carry definite helicities of  $\lambda_1$ ,  $\lambda_2$ , respectively. First let us imagine the process of a virtual photon decay into  $J/\psi$  and  $\chi_{cJ}$ . The differential decay rate can be expressed as [19, 20]

$$\frac{d\Gamma[\gamma^*(S_z) \rightarrow J/\psi(\lambda_1) + \chi_{cJ}(\lambda_2)]}{d\cos\theta} = \frac{|\mathbf{P}|}{16\pi s} |d_{S_z, \lambda}^1(\theta)|^2 |\mathcal{A}_{\lambda_1, \lambda_2}^J|^2, \quad (2.1)$$

where  $\lambda = \lambda_1 - \lambda_2$ ,  $S_z$  is the spin projection of the virtual photon along the  $\hat{z}$  axis.  $\mathcal{A}_{\lambda_1, \lambda_2}^J$  is the desired helicity amplitude, which encodes all the nontrivial dynamics. The angular

distribution is fully dictated by the quantum numbers  $S_z$  and  $\lambda$  through the Wigner rotation matrix  $d_{m,m'}^j(\theta)$ . Note angular momentum conservation constrains that  $|\lambda| \leq 1$ .

The number of independent helicity amplitudes can be greatly reduced, thanks to the parity invariance:

$$\mathcal{A}_{\lambda_1, \lambda_2}^J = (-1)^J \mathcal{A}_{-\lambda_1, -\lambda_2}^J. \quad (2.2)$$

Consequently, the two helicity amplitudes related by simultaneously flipping the helicities of  $J/\psi$  and  $\chi_{cJ}$  bear the equal magnitude.

It is straightforward to convert the differential decay rate (2.1) to the corresponding production cross section in  $e^+e^-$  annihilation:

$$\begin{aligned} \frac{d\sigma[e^+e^- \rightarrow J/\psi(\lambda_1) + \chi_{cJ}(\lambda_2)]}{d\cos\theta} &= \frac{2\pi\alpha}{s^{3/2}} \sum_{S_z=\pm 1} \frac{d\Gamma[\gamma^*(S_z) \rightarrow J/\psi(\lambda_1) + \chi_{cJ}(\lambda_2)]}{d\cos\theta} \\ &= \frac{\alpha}{8s^2} \left( \frac{|\mathbf{P}|}{\sqrt{s}} \right) |\mathcal{A}_{\lambda_1, \lambda_2}^J|^2 \times \begin{cases} \frac{1+\cos^2\theta}{2}, & (\lambda = \pm 1) \\ \sin^2\theta, & (\lambda = 0) \end{cases} \end{aligned} \quad (2.3)$$

where the polarizations of  $e^-$  and  $e^+$  have been averaged over. Note that we only need to sum over two *transverse* polarizations of the virtual photon, as guaranteed by the helicity conservation in QED for a massless electron. This selective summation is the cause for the anisotropic angular distribution patterns in (2.3).

It is now straightforward to acquire the unpolarized cross sections. Integrating (2.3) over the polar angle  $\theta$  and including all the allowed helicity states, one finally arrives at:

$$\sigma[J/\psi + \chi_{c0}] = \frac{\alpha}{6s^2} \left( \frac{|\mathbf{P}|}{\sqrt{s}} \right) \left( |\mathcal{A}_{0,0}^0|^2 + 2|\mathcal{A}_{1,0}^0|^2 \right), \quad (2.4a)$$

$$\sigma[J/\psi + \chi_{c1}] = \frac{\alpha}{6s^2} \left( \frac{|\mathbf{P}|}{\sqrt{s}} \right) \left( 2|\mathcal{A}_{1,0}^1|^2 + 2|\mathcal{A}_{0,1}^1|^2 + 2|\mathcal{A}_{1,1}^1|^2 \right), \quad (2.4b)$$

$$\sigma[J/\psi + \chi_{c2}] = \frac{\alpha}{6s^2} \left( \frac{|\mathbf{P}|}{\sqrt{s}} \right) \left( |\mathcal{A}_{0,0}^2|^2 + 2|\mathcal{A}_{1,0}^2|^2 + 2|\mathcal{A}_{0,1}^2|^2 + 2|\mathcal{A}_{1,1}^2|^2 + 2|\mathcal{A}_{1,2}^2|^2 \right) \quad (2.4c)$$

There are 2, 3 and 5 independent helicity amplitudes for  $\gamma^* \rightarrow J/\psi + \chi_{cJ}$  ( $J = 0, 1, 2$ ), respectively, as required by the angular momentum conservation. Note that parity transformation property (2.2) forbids the appearance of the  $\mathcal{A}_{0,0}^1$  amplitude. In equation (2.4), we include a factor of 2 to account for the parity-doublet contribution.

Aside from its great technical usefulness, the helicity amplitude formalism can also shed important light on the dynamics underlying exclusive reactions. In particular, each helicity amplitude possesses a definite power-law scaling in  $1/s$ , controlled by the *helicity selection rule* [21]. At asymptotically large  $\sqrt{s}$ , the polarized cross section for our double-charmonium production process scales as [8]:

$$\sigma[J/\psi(\lambda_1) + \chi_{cJ}(\lambda_2)] \sim \alpha^2 v^8 \left( \frac{m_c^2}{s} \right)^{2+|\lambda_1+\lambda_2|}, \quad (2.5)$$

here  $v$  denotes the characteristic velocity of charm quark inside a charmonium.

Equation (2.5), combined with angular momentum conservation, implies that the helicity state which exhibits the slowest asymptotic decrease, *i.e.*  $\sigma \propto 1/s^2$ , is the one that conserves

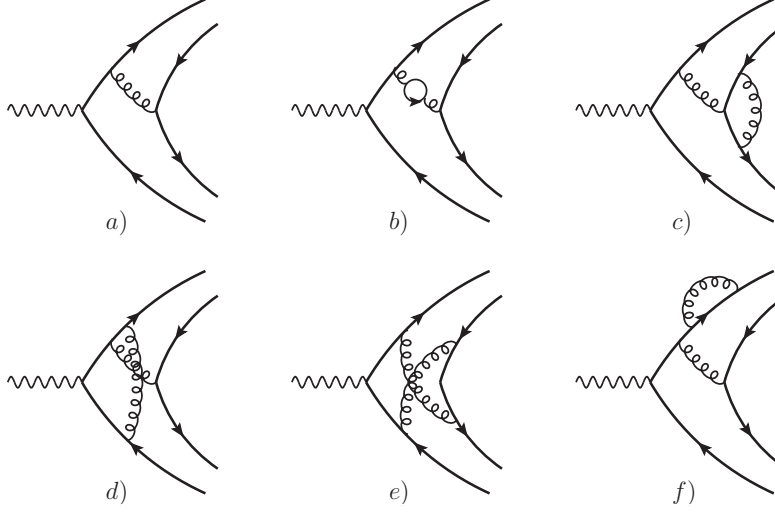


FIG. 1: One sample LO diagram and five sample NLO diagrams that contribute to  $\gamma^* \rightarrow J/\psi + \chi_{cJ}$ .

the hadron helicities  $|\lambda_1 + \lambda_2| = 0$ , or equivalently,  $(\lambda_1, \lambda_2) = (0, 0)$ . For each unit of the violation of this law, there is a further suppression factor of  $1/s$ . At sufficiently high energy, only the  $(0, 0)$  helicity state perhaps needs to be retained for phenomenological purposes. Note that in NRQCD factorization language, the charm quark is treated as heavy, and in fact its mass acts as the agent of violating the hadron helicity conservation.

Once beyond the lowest order in  $\alpha_s$ , the power-law scaling specified in (2.5) will in general receive mild modifications due to the  $\ln s$  terms. This logarithmic scaling violation will be examined in detail in Section 4.

### 3. LO PREDICTIONS FOR POLARIZED CROSS SECTIONS

At LO in  $v$  expansion in the NRQCD approach, one can factorize the amplitude of  $\gamma^* \rightarrow J/\psi + \chi_{cJ}$  as the product of the short-distance coefficients and the nonperturbative NRQCD matrix elements. To a good extent, these nonperturbative matrix elements are well approximated by the phenomenological (derivative of) wave function at the origin,  $R_{J/\psi}(0)$  and  $R'_{\chi_{cJ}}(0)$ . At LO in  $\alpha_s$ , the short-distance coefficients have been obtained [8, 9] by calculating the quark amplitude  $\gamma^* \rightarrow c\bar{c}(^3S_1^{(1)}) + c\bar{c}(^3P_J^{(1)})$  using the covariant projection technique [22, 23].

There are in total 4 Feynman diagrams at LO in  $\alpha_s$ , one of which is depicted in Fig. 1a). For simplicity, we have neglected the QED fragmentation diagrams, while their effect is modest. To expedite the extraction of the corresponding helicity amplitudes, we have constructed 10 helicity projection operators. It is convenient to parameterize the LO helicity amplitude as

$$\mathcal{A}_{\lambda_1, \lambda_2}^{J(0)} = \frac{4ee_c\alpha_s C_F R_{J/\psi}(0) R'_{\chi_{cJ}}(0)}{m_c^3} r^{\frac{1}{2}(1+|\lambda_1+\lambda_2|)} c_{\lambda_1, \lambda_2}^J(r), \quad (3.1)$$

where  $e_c = \frac{2}{3}$  is the electric charge of the charm quark, and for brevity, we have introduced

a dimensionless variable  $r$ :

$$r \equiv \frac{4m_c^2}{s}. \quad (3.2)$$

To make the scaling behavior in (2.5) transparent, we have explicitly stripped off a factor  $r^{\frac{1}{2}(1+|\lambda_1+\lambda_2|)}$  in (3.1), so that the reduced helicity amplitude  $c_{\lambda_1, \lambda_2}^J(r)$ , a dimensionless function, will start with a  $\mathcal{O}(1)$  constant. Concretely, these  $c_{\lambda_1, \lambda_2}^J(r)$  functions are

$$c_{0,0}^0(r) = 1 + 10r - 12r^2 \quad c_{1,0}^0(r) = 9 - 14r, \quad (3.3a)$$

$$c_{0,1}^1(r) = -\sqrt{6}(2 - 7r) \quad c_{1,0}^1(r) = -\sqrt{6}r \quad c_{1,1}^1(r) = -2\sqrt{6}(1 - 3r), \quad (3.3b)$$

$$c_{0,0}^2(r) = \sqrt{2}(1 - 2r - 12r^2) \quad c_{0,1}^2(r) = \sqrt{6}(1 - 5r) \quad c_{1,0}^2(r) = \sqrt{2}(3 - 11r), \\ c_{1,1}^2(r) = 2\sqrt{6}(1 - 3r) \quad c_{1,2}^2(r) = 2\sqrt{3}. \quad (3.3c)$$

These 10 helicity amplitudes agree with those given in Ref. [8]. It is interesting to note that the tree-level  $J/\psi(1) + \chi_{c1}(0)$  amplitude constitutes an exception in that it accidentally receives an extra suppression factor than expected from the helicity selection rule.

Plugging (3.1) into (2.4), we obtain the LO NRQCD predictions for the polarized cross sections:

$$\sigma^{(0)}[J/\psi(\lambda_1) + \chi_{cJ}(\lambda_2)] = \frac{32\pi e_c^2 \alpha^2 C_F^2 \alpha_s^2}{3s^2 m_c^6} \left( \frac{|\mathbf{P}|}{\sqrt{s}} \right) R_{J/\psi}^2(0) R_{\chi_{cJ}}^2(0) r^{1+|\lambda_1+\lambda_2|} |c_{\lambda_1, \lambda_2}^J(r)|^2. \quad (3.4)$$

## 4. NLO PERTURBATIVE CORRECTIONS TO POLARIZED CROSS SECTIONS

In this section, we first sketch some technical issues about the NLO perturbative calculations, then present the asymptotic expressions of the NLO corrections for all the encountered helicity amplitudes.

### A. Description of the calculation

We first employ the MATHEMATICA package FEYNARTS [24, 25] to generate Feynman diagrams and amplitudes for the parton process  $\gamma^* \rightarrow c\bar{c}(P_1) + c\bar{c}(P_2)$  to NLO in  $\alpha_s$ . Feynman gauge is used throughout this calculation. In total there are 20 two-point, 20 three-point, 18 four-point, and 6 five-point one-loop diagrams, some of which have been illustrated in Fig. 1. We then apply the covariant projector technique [22, 23] to enforce that two  $c\bar{c}$  pairs form the spin-triplet, color-singlet states, with the Dirac and color traces handled by the package FEYN CALC [26]. In the next step, we proceed to expand the integrand in powers of quark relative momenta,  $q$ , to project out the leading  $S$ -wave and  $P$ -wave orbital-angular-momentum contributions.

Making expansion in  $q$  prior to carrying out the loop integration, in the spirit of *method of region* [27], amounts to directly deducing the NRQCD short-distance coefficients, *i.e.*, the contributions solely stemming from the *hard* region ( $k^2 \geq m_c^2$ ). In practice, this procedure is far simpler than the conventional perturbative matching procedure, since by this way we will no longer be distracted by the effects from the low-energy regions, *e.g.*, from the *soft*

( $k^\mu \sim mv$ ), or *potential* ( $k^0 \sim mv^2$ ,  $|\mathbf{k}| \sim mv$ ) regions. Consequently, with this strategy, one will never confront Coulomb singularity in the one-loop integrals.

In Ref. [28], an all-order-in- $\alpha_s$  proof for exclusive quarkonium production has been outlined in the NRQCD factorization context. It is argued that, at lowest order in  $v$  and to all orders in  $\alpha_s$ , NRQCD factorization holds for  $S$ -wave plus  $P$ -wave quarkonia production in  $e^+e^-$  annihilation. In particular, this implies that the NRQCD short-distance coefficients associated with  $e^+e^- \rightarrow J/\psi + \chi_{cJ}$  should be free from any infrared singularity at NLO in  $\alpha_s$ <sup>1</sup>. Indeed, an earlier NLO perturbative calculation for  $e^+e^- \rightarrow J/\psi + \chi_{c0}$  has explicitly verified this pattern [16].

At this stage, we apply the specifically-designed helicity projection operators to project out 10 corresponding helicity amplitudes. This operation brings forth great simplification, for all the polarization vectors (tensors) have been eliminated, and the numerators in loop integrals now become the Lorentz scalars comprised entirely of external and loop momenta. Note these integrals in general contain propagators with quadratic power due to the projection of the  $P$ -wave state.

To proceed, we use the MATHEMATICA package FIRE [32] and our self-written MATHEMATICA code to reduce the general higher-point one-loop integrals into a set of Master Integrals (MI). Fortunately, as a great bonus of having Taylor-expanded the integrand in powers of  $q$ , together with having applied the helicity projectors, there are only three linearly-independent Lorentz scalars in loop integrals:  $l^2$ ,  $l \cdot P_1$  and  $l \cdot P_2$ , where  $l$ ,  $P_1$ ,  $P_2$  stand for the loop momentum, the momenta carried by the  $c\bar{c}(^3S_1^{(1)})$  pair and by the  $c\bar{c}(^3P_J^{(1)})$  pair, respectively. Thanks to the integration-by-part algorithm built in FIRE, it turns out that all the involved MI become just the usual 2-point and 3-point scalar integrals. All the encountered 3-point scalar integrals can be found in Appendix of Ref. [12]. We have used the package LOOPTOOLS [33] to numerically check the correctness of these integrals.

Throughout this calculation we adopt dimensional regularization to regularize both the ultraviolet (UV) and infrared (IR) singularities. In accordance with the LSZ reduction formula, one needs to multiply the tree-level amplitude by  $(\sqrt{Z_c})^4$ , where  $Z_c$  denotes the residue of the charm quark propagator near its pole. This contribution is represented by Fig. 1f). In Feynman gauge, the residue is given by

$$Z_c = 1 - C_F \frac{\alpha_s}{4\pi} \left[ \frac{1}{\epsilon_{\text{UV}}} + \frac{2}{\epsilon_{\text{IR}}} - 3\gamma_E + 3 \ln \frac{4\pi\mu^2}{m_c^2} + 4 \right] + \mathcal{O}(\alpha_s^2), \quad (4.1)$$

where  $\gamma_E$  is the Euler constant, and  $C_F = \frac{N_c^2 - 1}{2N_c}$ .

In addition, we also need to replace the bare charm quark mass and the bare QCD

---

<sup>1</sup> An uncanceled infrared singularity has been discovered in NLO calculation for the  $B \rightarrow K\chi_{cJ}$  [29, 30], which has been interpreted as a failure of NRQCD factorization. This symptom hints that the lower-energy degrees of freedom, the *ultrasoft* ( $k \sim mv^2$ ) region, has been erroneously missed, and one should invoke the even lower energy effective theory, the potential NRQCD, to remedy this problem. Once the ultrasoft mode from higher Fock state  $|c\bar{c}(^3S_1^{(8)})g\rangle$  is consistently taken into account, this infrared divergence can be tamed [31].

coupling constant in the tree-level amplitude by

$$m_c^{\text{bare}} = m_c \left[ 1 - 3C_F \frac{\alpha_s}{4\pi} \left( \frac{1}{\epsilon_{\text{UV}}} - \gamma_E + \ln \frac{4\pi\mu^2}{m_c^2} + \frac{4}{3} \right) + \mathcal{O}(\alpha_s^2) \right], \quad (4.2a)$$

$$\alpha_s^{\text{bare}} = \alpha_s(\mu)^{\overline{\text{MS}}} \left[ 1 - \beta_0 \frac{\alpha_s}{4\pi} \left( \frac{1}{\epsilon_{\text{UV}}} - \gamma_E + \ln(4\pi) \right) + \mathcal{O}(\alpha_s^2) \right]. \quad (4.2b)$$

where  $\beta_0 = \frac{11}{3}N_c - \frac{2}{3}n_f$  is the one-loop coefficient of the QCD  $\beta$  function, and  $n_f = 4$  denotes the number of active quark flavors.

When adding the contributions from all the diagrams, we find that the ultimate NLO expressions for each of the 10 helicity amplitudes are UV and IR finite.

## B. Analytic expressions of NLO helicity amplitudes

For clarity, we parameterize the NLO helicity amplitude as follows:

$$\mathcal{A}_{\lambda_1, \lambda_2}^{J(1)} = \frac{\alpha_s}{\pi} K_{\lambda_1, \lambda_2}^J \left( r, \frac{\mu^2}{s} \right) \mathcal{A}_{\lambda_1, \lambda_2}^{J(0)}, \quad (4.3)$$

where the LO helicity amplitude  $\mathcal{A}^{(0)}$  is defined in (3.1). The dimensionless quantity  $K_{\lambda_1, \lambda_2}^J$ , a function of  $r$  and the renormalization scale  $\mu$ , can be regarded as the reduced NLO helicity amplitude. It necessarily encompasses all the loop dynamics. Since helicity selection rule has been tacitly embodied in  $\mathcal{A}^{(0)}$  in (4.3), we expect that the  $K$  functions will exhibit slower asymptotic decrease than any power-law scaling in  $r$ .

The reduced NLO helicity amplitudes  $K$  are in general complex-valued. Their analytic expressions are somewhat lengthy and will not be reproduced here. On the other hand, in Figs. 2, 3, and 4, we explicitly display their profiles over a wide range of  $r$  for each of the 10 helicity amplitudes.

Combining (3.1), (4.3) and (2.4), we can deduce the NLO perturbative correction to the polarized cross section:

$$\sigma^{(1)}[J/\psi(\lambda_1) + \chi_{cJ}(\lambda_2)] = 2 \left( \frac{\alpha_s}{\pi} \right) \text{Re} \left\{ K_{\lambda_1, \lambda_2}^J \left( r, \frac{\mu^2}{s} \right) \right\} \sigma^{(0)}[J/\psi(\lambda_1) + \chi_{cJ}(\lambda_2)], \quad (4.4)$$

where  $\sigma^{(0)}$  is given in (3.4). To the desired NLO accuracy, the imaginary part of the  $K$  function does not contribute. We now have improved prediction  $\sigma_{\text{NLO}} = \sigma^{(0)} + \sigma^{(1)}$ .

It is theoretically curious to know the asymptotic behaviors of these reduced helicity amplitudes in the limit  $\sqrt{s} \gg m_c$ . As was mentioned before, we anticipate to see the logarithmic scaling violation at NLO to the naive power-law scaling rule (2.5). Moreover, performing the asymptotic expansion in NRQCD short-distance coefficients is theoretically very appealing, since it is equivalent to disentangling the effects occurring at the “hard” scale (virtuality  $\sim s$ ) from the lower-energy “collinear/soft” effects (virtuality  $\sim m_c^2$ ), by which one can intimately link the NRQCD factorization approach and the light-cone approach [18, 34]. Such asymptotic expansion has been carried out for several double-quarkonium production processes at one-loop level [18, 35, 36] and some general patterns have been recognized.



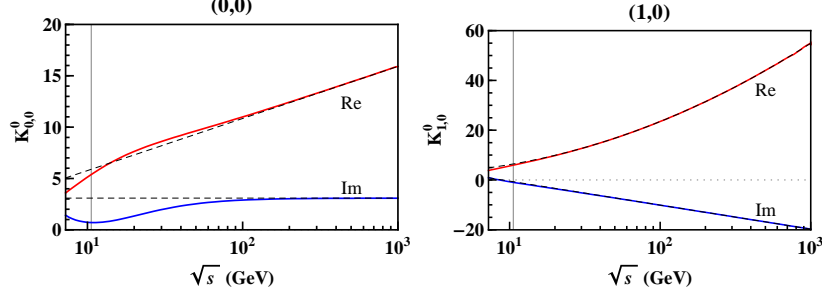


FIG. 2: The profiles of two reduced NLO helicity amplitudes  $K_{\lambda_1, \lambda_2}^0$  (for  $\gamma^* \rightarrow J/\psi + \chi_{c0}$ ) with  $\sqrt{s}$  varied in a wide range. We take  $\mu = \frac{\sqrt{s}}{2}$  and  $m_c = 1.5$  GeV. The solid curves correspond to the exact results, and the dashed curves represent the asymptotic ones as given in (4.5). The vertical mark is placed at the  $B$  factory energy  $\sqrt{s} = 10.58$  GeV.

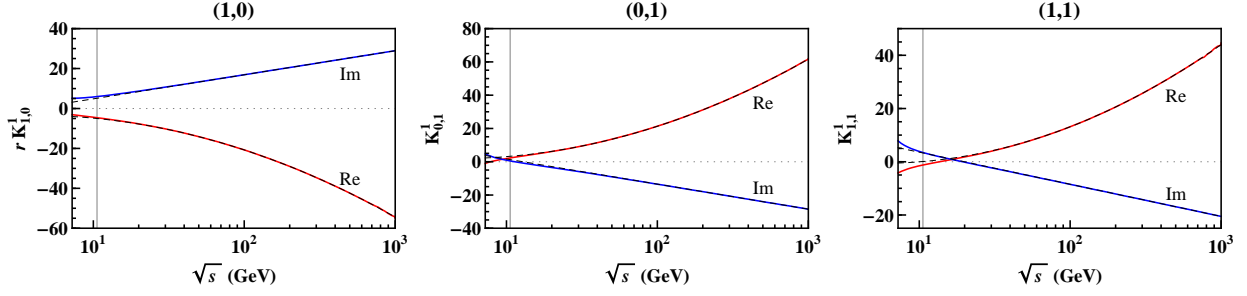


FIG. 3: The profiles of three reduced NLO helicity amplitudes  $K_{\lambda_1, \lambda_2}^1$  (for  $\gamma^* \rightarrow J/\psi + \chi_{c1}$ ). The asymptotic curves are taken from (4.6). The parameters are the same as in Fig. 2.

The asymptotic expressions of two reduced NLO helicity amplitudes for  $J/\psi + \chi_{c0}$  are

$$K_{0,0}^0 \left( r, \frac{\mu^2}{s} \right)_{\text{asym}} = -\frac{1}{3}(4 - \ln 2) \ln r + \frac{\beta_0}{4} \left( \ln \frac{4\mu^2}{s} + \frac{8}{3} \right) - \frac{1}{18}(46 + \pi^2 - 40 \ln 2 + 33 \ln^2 2) + \frac{i\pi}{4} \left( \beta_0 - \frac{16}{3} + \frac{4}{3} \ln 2 \right), \quad (4.5a)$$

$$K_{1,0}^0 \left( r, \frac{\mu^2}{s} \right)_{\text{asym}} = \frac{1}{3} \ln^2 r - \frac{1}{108}(139 - 104 \ln 2) \ln r + \frac{\beta_0}{4} \left( \ln \frac{4\mu^2}{s} + \frac{17}{9} \right) - \frac{1}{54} \left( 161 + \frac{8\pi^2}{3} - \frac{495}{2} \ln 2 + 100 \ln^2 2 \right) + \frac{i\pi}{4} \left( \frac{8}{3} \ln r + \beta_0 - \frac{1}{27}(139 - 104 \ln 2) \right). \quad (4.5b)$$

The asymptotic expressions of the three reduced NLO helicity amplitudes for  $J/\psi + \chi_{c1}$

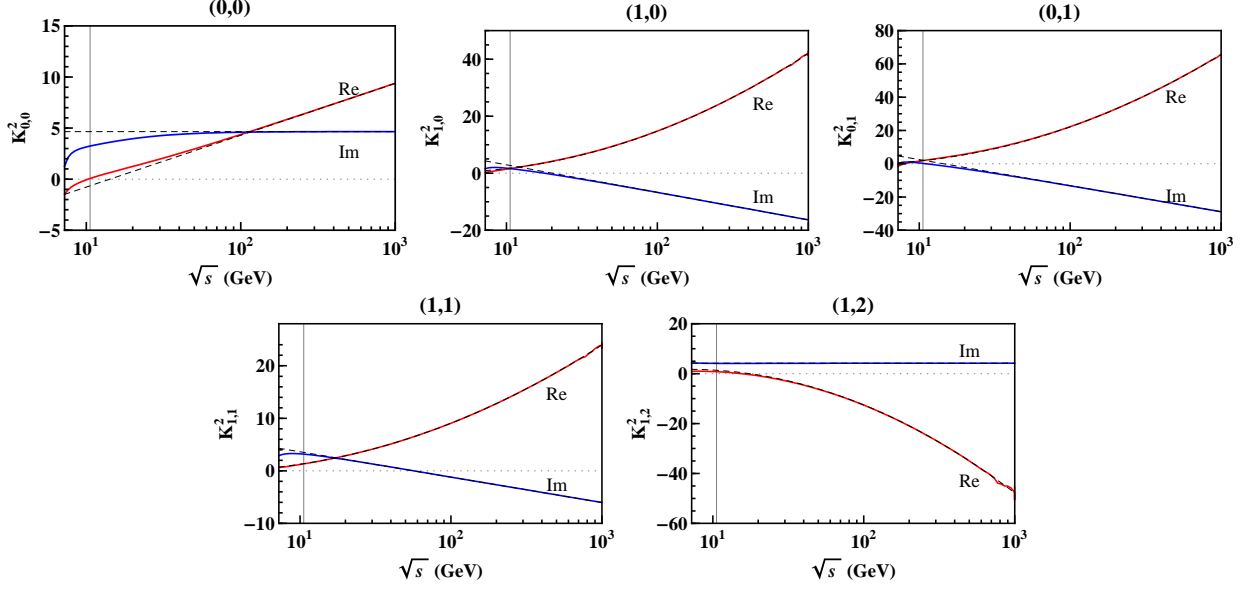


FIG. 4: The profiles of five reduced NLO helicity amplitudes  $K_{\lambda_1, \lambda_2}^2$  (for  $\gamma^* \rightarrow J/\psi + \chi_{c2}$ ). The asymptotic curves are taken from (4.7). The parameters are the same as in Fig. 2.

read

$$r K_{1,0}^1 \left( r, \frac{\mu^2}{s} \right)_{\text{asym}} = -\frac{1}{12} \left\{ 5 \ln^2 r + (7 - 2 \ln 2) \ln r - 19 + 2\pi^2 + 75 \ln 2 - 21 \ln^2 2 \right. \\ \left. + i\pi(10 \ln r + 7 - 2 \ln 2) \right\}, \quad (4.6a)$$

$$K_{0,1}^1 \left( r, \frac{\mu^2}{s} \right)_{\text{asym}} = \frac{1}{24} \left\{ \frac{25}{2} \ln^2 r - (46 - 99 \ln 2) \ln r + 6\beta_0 \left( \ln \frac{4\mu^2}{s} + \frac{13}{6} \right) \right. \\ \left. - \frac{1}{6}(616 + 74\pi^2 - 1696 \ln 2 + 303 \ln^2 2) + i\pi(25 \ln r + 6\beta_0 - 46 + 99 \ln 2) \right\}, \quad (4.6b)$$

$$K_{1,1}^1 \left( r, \frac{\mu^2}{s} \right)_{\text{asym}} = \frac{1}{24} \left\{ 10 \ln^2 r + 2(1 + 17 \ln 2) \ln r + 6\beta_0 \left( \ln \frac{4\mu^2}{s} + \frac{13}{6} \right) \right. \\ \left. - \frac{1}{3}(266 + 7\pi^2 - 128 \ln 2 + 147 \ln^2 2) + 2i\pi(10 \ln r + 3\beta_0 + 1 + 17 \ln 2) \right\}. \quad (4.6c)$$

The asymptotic expressions of the five reduced NLO helicity amplitudes for  $J/\psi + \chi_{c2}$

are

$$K_{0,0}^2 \left( r, \frac{\mu^2}{s} \right)_{\text{asym}} = -\frac{1}{3}(4 - \ln 2) \ln r + \frac{\beta_0}{4} \left( \ln \frac{4\mu^2}{s} + \frac{8}{3} \right) - \frac{1}{18}(64 + \pi^2 + 104 \ln 2 + 33 \ln^2 2) + \frac{i\pi}{4} \left( \beta_0 - \frac{10}{3} + \frac{4}{3} \ln 2 \right), \quad (4.7a)$$

$$K_{0,1}^2 \left( r, \frac{\mu^2}{s} \right)_{\text{asym}} = \frac{1}{12} \left\{ \frac{13}{2} \ln^2 r - (22 - 43 \ln 2) \ln r + 3\beta_0 \left( \ln \frac{4\mu^2}{s} + \frac{8}{3} \right) - \frac{1}{6}(284 + 30\pi^2 - 380 \ln 2 + 159 \ln^2 2) + i\pi(13 \ln r + 3\beta_0 - 14 + 43 \ln 2) \right\}, \quad (4.7b)$$

$$K_{1,0}^2 \left( r, \frac{\mu^2}{s} \right)_{\text{asym}} = \frac{1}{6} \left\{ 2 \ln^2 r + \frac{1}{6}(5 + 8 \ln 2) \ln r + \frac{3}{2}\beta_0 \left( \ln \frac{4\mu^2}{s} + \frac{7}{3} \right) - \frac{1}{18}(291 - 8\pi^2 + 171 \ln 2 + 312 \ln^2 2) + i\pi \left( 4 \ln r + \frac{3}{2}\beta_0 + \frac{11}{6} + \frac{4}{3} \ln 2 \right) \right\}, \quad (4.7c)$$

$$K_{1,1}^2 \left( r, \frac{\mu^2}{s} \right)_{\text{asym}} = \frac{1}{24} \left\{ 4 \ln^2 r - (46 - 62 \ln 2) \ln r + 6\beta_0 \left( \ln \frac{4\mu^2}{s} + \frac{13}{6} \right) - \frac{1}{3}(274 + 27\pi^2 - 316 \ln 2 + 9 \ln^2 2) + i\pi(8 \ln r + 6\beta_0 - 46 + 62 \ln 2) \right\}, \quad (4.7d)$$

$$K_{1,2}^2 \left( r, \frac{\mu^2}{s} \right)_{\text{asym}} = -\frac{1}{4} \left\{ 2 \ln^2 r + \frac{2}{3}(1 + 13 \ln 2) \ln r - \beta_0 \left( \ln \frac{4\mu^2}{s} + \frac{5}{3} \right) + \frac{1}{9}(-7\pi^2 + 140 - 104 \ln 2 + 237 \ln^2 2) - i\pi \left( \beta_0 + 3 - \frac{26}{3} \ln 2 \right) \right\}. \quad (4.7e)$$

Now we can make several interesting observations from Eqs. (4.5), (4.6), (4.7). One confirms that the scaling violation is indeed of the logarithmic form. For the hadron-helicity-conserving channels such as  $J/\psi(0) + \chi_{c0,2}(0)$ , the leading scaling behavior of the real part of the  $K$  function is governed by a single logarithm of  $r$ ; for all the remaining helicity-suppressed channels, the leading asymptotic behaviors of the respective  $K$  functions are all proportional to  $\ln^2 r$ .

This pattern lends further support for the speculation made in Ref. [18]: The hard exclusive processes involving double-quarkonium at leading twist can only accommodate the single collinear logarithm at one-loop, while those beginning with the higher twist contributions are always plagued with double logarithms. For example, the NLO NRQCD short-distance coefficients of the helicity-suppressed reactions  $e^+e^- \rightarrow J/\psi + \eta_c$  and  $\eta_b \rightarrow J/\psi J/\psi$  are both found to contain the double-logarithm term [18, 36].

Most of the studied double-charmonium production processes are of the helicity-suppressed type. In this regard, the helicity channels  $e^+e^- \rightarrow J/\psi(0) + \chi_{c0,2}(0)$  constitute the rather rare examples that the leading-twist contribution dominates. In such a situation, by resorting to the leading-twist collinear factorization theorem, one can employ the light-cone approach to efficiently reproduce the asymptotic expressions given in (4.5a) and (4.7a), very much like what is achieved for  $B_c$  electromagnetic form factor at NLO in  $\alpha_s$  [18]. Note

that the single logarithm in these two channels have identical coefficient  $\propto 4 - \ln 2$ . This coefficient can be readily reconstructed in light-cone approach, with the aid of the Efremov-Radyushkin-Brodsky-Lepage (ERBL) evolution equation [37, 38]. Moreover, following the strategy of [34], by employing this evolution equation, one can systematically identify and resum the leading collinear logarithms in these amplitudes to all orders in  $\alpha_s$ .

In contrast, it remains to be an open challenge for light-cone approach to reproduce these process-dependent double logarithms appearing in NLO NRQCD short-distance coefficients, which seem to have resulted from the overlap between collinear and endpoint singularities [18]. Note that the end-point singularity is a long-standing problem in light-cone framework, which has essentially hindered our capability of performing the complete NLO perturbative calculation beyond leading-twist using this approach. Perhaps the first major progress is to successfully reproduce the asymptotic expressions related with those  $(0, 1)$  and  $(1, 0)$  helicity channels, where only twist-3 effects need be considered.

For reader's convenience, all the asymptotic results of the reduced helicity amplitudes are also shown in Figs. 2, 3, 4, in juxtapose with the corresponding exact NLO results. As can be seen clearly, for those higher-twist helicity channels, the asymptotic results tend to converge with the exact ones decently well at relatively lower  $\sqrt{s}$  (say, at  $B$  factory energy) than for the leading-twist channels. This seems to be a general feature, which has also been observed in several other double charmonium production processes [18, 35, 36].

To conclude this section, we mention a peculiar phenomenon affiliated with the helicity channel  $\gamma^* \rightarrow J/\psi(1) + \chi_{c1}(0)$ . Recall that this helicity amplitude at LO has been suppressed by an unwanted factor of  $r$ , as can be seen in (3.3b). Nevertheless, as one may readily tell from (4.6a), at NLO in  $\alpha_s$ , this helicity amplitude recovers the correct power-law scaling as dictated by the helicity selection rule! This implies that at very high energy, the NLO contribution is far more significant than the LO piece for this helicity channel, despite its extra suppression by  $\alpha_s$ . It might be also worth noting that, unlike all the other asymptotic expressions, the renormalization logarithm  $\beta_0 \ln \mu^2/s$  is absent in (4.6a). This is very similar to what is found in NLO perturbative correction to  $\eta_b \rightarrow J/\psi J/\psi$  [36].

## 5. PHENOMENOLOGY

With our NLO calculations completed, following the formulas (3.4) and (4.4), we are ready to carry out a detailed analysis for the processes  $e^+e^- \rightarrow J/\psi(\psi') + \chi_{cJ}$  and confront the  $B$  factory measurements. In our numerical analysis, we set  $\sqrt{s} = 10.58$  GeV,  $m_c = 1.5$  GeV. The electromagnetic fine structure constant is chosen as  $\alpha(\sqrt{s}) = 1/130.9$  [39]. The running QCD strong coupling constant is evaluated by using the two-loop formula with  $\Lambda_{\overline{\text{MS}}}^{(4)} = 0.338$  GeV [11, 12]. The nonperturbative input parameters, *i.e.*, the wave function at the origin for  $J/\psi(\psi')$ , as well as the first derivative of the radial wave function at the origin for  $\chi_{cJ}$ , bear a fair amount of uncertainties. Their values have been compiled in Ref. [40], which are estimated from several different potential models. We choose to use those given by the Buchmüller-Tye potential model [41]:  $|R_{J/\psi}(0)|^2 = 0.81$  GeV<sup>3</sup>,  $|R_{\psi'}(0)|^2 = 0.529$  GeV<sup>3</sup>, and  $|R'_{\chi_{cJ}}(0)|^2 = 0.075$  GeV<sup>5</sup>.

Another important source of uncertainty for the NLO predictions comes from the scale setting for the strong coupling constant. As is well known, this scale ambiguity is a typical nuisance of NRQCD factorization approach, reflecting the fact that two disparate hard scales,  $\sqrt{s}$  and  $m_c$ , are entangled together in NRQCD short-distance coefficients. In contrast, the

light-cone approach, when armed with the idea of refactorization, can efficiently disentangle these two scales, so one naturally expects that the scale ambiguity will be greatly reduced.

While it may sound natural to choose the renormalization scale  $\mu$  to be around the highest scale  $\sqrt{s}$ , however, as is clearly illustrated in [18], it is rather unappealing to set the scales entering all  $\alpha_s$  in NLO short-distance coefficient to be around  $\sqrt{s}$  unanimously. The reason is that a part of NLO correction comes from the loop region with lower virtuality, and as such can be identified with the NLO perturbative correction to the charmonium decay constant, so the corresponding  $\alpha_s$  should definitely be affiliated with a scale around  $2m_c$  rather than  $\sqrt{s}$ .

Since it is not possible to completely solve the scale ambiguity problem within the confines of the NRQCD factorization approach, we proceed to estimate the cross section by assigning all the occurring  $\alpha_s$  with a common scale,  $\mu$ , and choosing  $\mu = \sqrt{s}/2$  and  $\mu = 2m_c$ , respectively. It is hoped that the less biased results interpolate between these two sets of predictions.

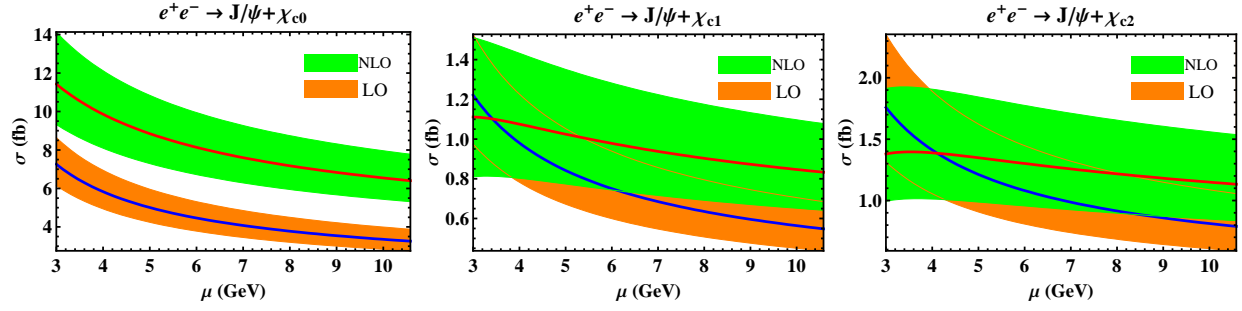


FIG. 5: The  $\mu$ -dependence of LO and NLO cross sections for  $e^+e^- \rightarrow J/\psi + \chi_{cJ}$  ( $J = 0, 1, 2$ ) at  $\sqrt{s} = 10.58$  GeV. The uncertainty band is due to sliding  $m_c$  between 1.4 GeV and 1.6 GeV, where the central curves correspond to  $m_c = 1.5$  GeV.

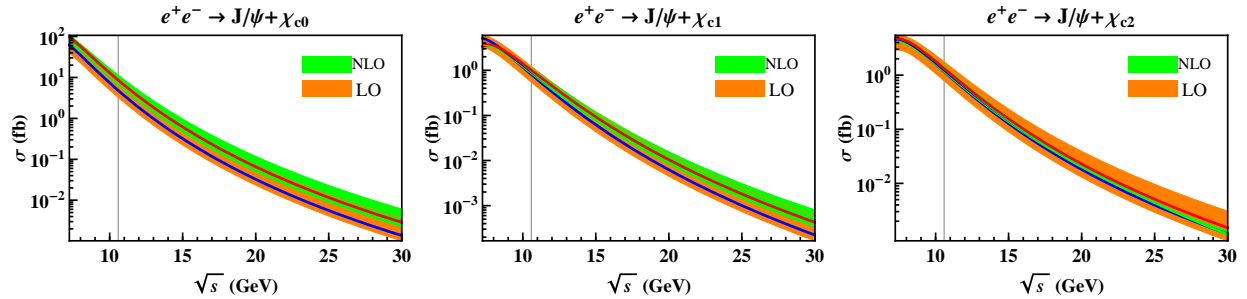


FIG. 6: The LO and NLO cross sections for  $e^+e^- \rightarrow J/\psi + \chi_{cJ}$  ( $J = 0, 1, 2$ ) as a function of  $\sqrt{s}$ . The uncertainty band is obtained by varying  $\mu$  from  $2m_c$  to  $\sqrt{s}$ , where the central curves represent the default choice  $\mu = \frac{\sqrt{s}}{2}$ .

To develop a concrete feel about the scale dependence, in Fig. 5 we explicitly show the  $\mu$ -dependence of the LO and NLO total cross sections for the processes  $e^+e^- \rightarrow J/\psi + \chi_{cJ}$  ( $J = 0, 1, 2$ ) at  $B$  factory energy. As can be clearly seen, including the NLO correction has notably reduced the scale dependence for  $J/\psi + \chi_{c1,2}$ , whereas of little impact for  $J/\psi + \chi_{c0}$ .

TABLE 1: Polarized cross sections for each helicity channel and unpolarized (total) cross sections (in unit of fb) for  $e^+e^- \rightarrow J/\psi + \chi_{cJ}$  ( $J = 0, 1, 2$ ). In the rightmost column, we also list the K factor for the unpolarized cross sections. We choose the following input parameters:  $m_c = 1.5$  GeV,  $\mu = \sqrt{s}/2$ , accordingly,  $\alpha_s(\mu) = 0.211$ .

		$\sigma_{(0,0)}$	$\sigma_{(1,0)}$	$\sigma_{(0,1)}$	$\sigma_{(1,1)}$	$\sigma_{(1,2)}$	$\sigma_{\text{tot}}$	K
$J/\psi + \chi_{c0}$	LO	1.11	1.86	–	–	–	4.83	1.79
	NLO	1.92	3.35	–	–	–	8.62	
$J/\psi + \chi_{c1}$	LO	–	0.0012	0.37	0.033	–	0.81	1.24
	NLO	–	–0.0078	0.49	0.028	–	1.01	
$J/\psi + \chi_{c2}$	LO	0.43	0.27	0.064	0.033	0.0023	1.17	1.14
	NLO	0.44	0.33	0.081	0.039	0.0026	1.33	

TABLE 2: The same as Table 1, except we choose the different renormalization scale:  $\mu = 2m_c$ , accordingly  $\alpha_s(\mu) = 0.259$ .

		$\sigma_{(0,0)}$	$\sigma_{(1,0)}$	$\sigma_{(0,1)}$	$\sigma_{(1,1)}$	$\sigma_{(1,2)}$	$\sigma_{\text{tot}}$	K
$J/\psi + \chi_{c0}$	LO	1.67	2.80	–	–	–	7.26	1.57
	NLO	2.50	4.46	–	–	–	11.43	
$J/\psi + \chi_{c1}$	LO	–	0.0017	0.56	0.050	–	1.22	0.91
	NLO	–	–0.016	0.55	0.020	–	1.11	
$J/\psi + \chi_{c2}$	LO	0.65	0.40	0.097	0.050	0.0035	1.76	0.78
	NLO	0.40	0.35	0.089	0.041	0.0026	1.38	

Also in Fig. 5 we have examined the  $m_c$ -dependence of the cross section, which is reflected in the error band by varying  $m_c$  from 1.4 GeV and 1.6 GeV.

In Fig. 6, we also plot the LO and NLO total cross sections for  $e^+e^- \rightarrow J/\psi + \chi_{cJ}$  ( $J = 0, 1, 2$ ) as a function of  $\sqrt{s}$ . The error band is obtained by sliding  $\mu$  from  $2m_c$  to  $\sqrt{s}$ , where the central curves represent the default choice  $\mu = \frac{\sqrt{s}}{2}$ . For the LO predictions, all the  $J/\psi + \chi_{cJ}$  channels have comparable widths of the error bands. But the NLO results for  $J/\psi + \chi_{c2}$  exhibit a significantly narrower band compared to those for  $J/\psi + \chi_{c0,1}$ .

Table 1 and Table 2 tabulate our predictions to both of the LO and NLO cross sections for  $e^+e^- \rightarrow J/\psi + \chi_{cJ}$  ( $J = 0, 1, 2$ ), with these two sets of  $\mu$  chosen respectively. In addition to the unpolarized (total) cross sections, we also include the polarized cross sections from each helicity channel.

Let us first discuss the unpolarized cross sections. For  $e^+e^- \rightarrow J/\psi + \chi_{c0}$ , the NLO correction has significantly enhanced the LO prediction, with a K factor of 1.79 and 1.57 respectively, corresponding to two different choices of  $\mu$ <sup>2</sup>. In contrast, the NLO corrections

<sup>2</sup> We find disagreement with the previous NLO correction calculation for  $e^+e^- \rightarrow J/\psi + \chi_{c0}$  [16]. When taking the same input parameters as theirs, we obtain the K factor of 1.57, while theirs is 2.8.

TABLE 3: Comparison between our predicted unpolarized cross sections with the measurements at B factories for  $e^+e^- \rightarrow J/\psi(\psi') + \chi_{cJ}$  ( $J = 0, 1, 2$ ). The cross sections are in units of fb. We fix  $m_c = 1.5$  GeV, the error is estimated by varying  $\mu$  from  $2m_c$  to  $\sqrt{s}$ , where the central value refers to  $\mu = \sqrt{s}/2$ .

	BELLE $\sigma \times \mathcal{B}_{>2(0)}[42]$	BABAR $\sigma \times \mathcal{B}_{>2}[6]$	LO prediction	NLO prediction
$\sigma(J/\psi + \chi_{c0})$	$6.4 \pm 1.7 \pm 1.0$	$10.3 \pm 2.5^{+1.4}_{-1.8}$	$4.83^{+2.43}_{-1.57}$	$8.62^{+2.80}_{-2.22}$
$\sigma(J/\psi + \chi_{c1})$	-	-	$0.81^{+0.41}_{-0.26}$	$1.01^{+0.10}_{-0.18}$
$\sigma(J/\psi + \chi_{c2})$	-	-	$1.17^{+0.59}_{-0.38}$	$1.33^{+0.04}_{-0.20}$
$\sigma(J/\psi + \chi_{c1}) + \sigma(J/\psi + \chi_{c2})$	$< 5.3$ at 90% CL	-	$1.98^{+1.00}_{-0.64}$	$2.35^{+0.14}_{-0.38}$
$\sigma(\psi' + \chi_{c0})$	$12.5 \pm 3.8 \pm 3.1$	-	$2.79^{+1.41}_{-0.91}$	$4.98^{+1.62}_{-1.28}$
$\sigma(\psi' + \chi_{c1})$	-	-	$0.47^{+0.24}_{-0.15}$	$0.58^{+0.06}_{-0.10}$
$\sigma(\psi' + \chi_{c2})$	-	-	$0.68^{+0.34}_{-0.22}$	$0.77^{+0.03}_{-0.12}$
$\sigma(\psi' + \chi_{c1}) + \sigma(\psi' + \chi_{c2})$	$< 8.6$ at 90% CL	-	$1.14^{+0.58}_{-0.37}$	$1.36^{+0.08}_{-0.22}$

to  $e^+e^- \rightarrow J/\psi + \chi_{c1,2}$  have a milder impact, even with the sign uncertain. Concretely speaking, the first setting of  $\mu$  tends to increase the LO results modestly, while the second setting tends to reduce the LO results to some extent. This behavior may be clearly seen in Fig. 5. There the LO and NLO prediction bands cross with each other for  $e^+e^- \rightarrow J/\psi + \chi_{c1,2}$ , which implies that the  $K$  factor could be above or below 1, depending on the chosen scale. A similar understanding can also be achieved in Fig. 6. At  $\sqrt{s} = 10.58$  GeV, one sees from Fig. 6 the uncertainty band of the NLO predictions for  $e^+e^- \rightarrow J/\psi + \chi_{c1,2}$  has been completely submerged inside the band of the LO predictions. Therefore, depending on whether choosing the lower or upper bound for LO cross section, the  $K$  factor would be greater or less than 1.

In Table 3, we compare our predicted cross sections with the measurements at B factories for  $e^+e^- \rightarrow J/\psi(\psi') + \chi_{cJ}$  ( $J = 0, 1, 2$ ). One sees that the NLO perturbative correction to  $J/\psi + \chi_{c0}$  really brings the NRQCD prediction closer to the data, although there exists some slight tension between BABAR and BELLE measurements. By far, the  $e^+e^- \rightarrow J/\psi(\psi') + \chi_{c1,2}$  processes have not yet been observed in any experiments. Our predictions for the  $J/\psi(\psi') + \chi_{c1,2}$  cross sections are compatible with the upper bounds placed by the BELLE experiment. However, even if the large positive NLO correction is taken into account, our predicted  $\psi' + \chi_{c0}$  cross section is still significantly below the central value of the BELLE measurement. To clarify this puzzling situation, it seems necessary, and, urgent, for BABAR to perform an independent measurement for this process to see whether it confirms or disconfirms the BELLE results.

It seems foreseeable that, in future Super  $B$  factory, experimentalists may be able to measure some of the polarized cross sections for the  $e^+e^- \rightarrow J/\psi + \chi_{cJ}$  processes. Therefore, it is informative to examine the polarized cross sections in Table 1 and Table 2.

For  $J/\psi + \chi_{c0}$  production cross section, both the (0,0) and (1,0) helicity channels have comparable magnitude, either at LO or at NLO, and the latter is even somewhat greater. This is quite counterintuitive, diametrically contradicting what is expected from the helicity selection rule. This might be viewed as a hint that the  $B$  factory energy may lie still far

from the asymptotic scaling regime.

For  $e^+e^- \rightarrow J/\psi + \chi_{c1}$ , the hierarchy among the cross sections of three different helicity channels is also somewhat abnormal. The contribution from the  $(0, \pm 1)$  channel is far more significant than the other two, and to a good approximation, one only needs to retain this channel. This pattern still holds true after incorporating the NLO correction for both settings of  $\mu$ . It will be interesting for future Super  $B$  experiments to verify that the angular distribution of  $J/\psi$  (or  $\chi_{c1}$ ) is predominantly of form  $1 + \cos^2 \theta$ . In passing, we also note that the tiny LO contribution from the  $(\pm 1, 0)$  state may be attributable to the accidental suppression factor with respect to the helicity selection rule. After including the NLO correction,  $\sigma_{(1,0)}$  even becomes negative. This can be easily understood by inspecting (4.6a), since the NLO helicity amplitude is  $1/r$  enhanced relative to the LO one, and with opposite sign. However, in practice this polarized cross section is too small to be measured.

For  $e^+e^- \rightarrow J/\psi + \chi_{c2}$ , the hierarchy among the cross sections of five different helicity channels roughly obeys the helicity selection rule, except the contribution from the  $(0, \pm 1)$  channel is much smaller than the  $(\pm 1, 0)$  channel. From Table 1 and Table 2, one sees that the bulk of the cross sections comes from only two helicity states, *i.e.*  $(0, 0)$  and  $(\pm 1, 0)$ . For  $\mu = \sqrt{s}/2$ , the NLO correction has small impact on both helicity states; for  $\mu = 2m_c$ , the NLO corrections push down both polarized cross sections to some extent. It would be interesting for the future high-statistics experiment to observe this production process, and test whether the produced  $\chi_{c2}$  are predominantly longitudinally-polarized.

## 6. SUMMARY

In this work we have computed the complete NLO perturbative corrections to  $e^+e^- \rightarrow J/\psi + \chi_{cJ}$  ( $J = 0, 1, 2$ ) within the NRQCD factorization framework. The NLO NRQCD short-distance coefficients are inferred by directly extracting the contribution from the *hard* loop-momentum region. We have calculated the NLO corrections to each of the 10 independent helicity amplitudes. We have made a detailed analysis for both the polarized and unpolarized cross sections and compared with the measurements at  $B$  factory.

We find a significant positive NLO perturbative correction to  $e^+e^- \rightarrow J/\psi + \chi_{c0}$ , which helps to bring the predicted cross section in agreement with the  $B$  factory measurements. In contrast, our NLO predictions to  $\psi' + \chi_{c0}$  cross section is still significantly below the central value of the BELLE measurement. It is still too early to draw any solid conclusion about whether NRQCD factorization fails for this channel or not. We perhaps need to wait until BABAR collaboration carries out an independent measurement for this process.

The impact of NLO corrections to  $e^+e^- \rightarrow J/\psi + \chi_{c1,2}$  seems to be rather mild, even with their signs uncertain. Notice the predicted cross sections for these processes are about 5 or 6 times smaller than that for  $e^+e^- \rightarrow J/\psi + \chi_{c0}$ . Hopefully the future Super  $B$  factory, with much higher luminosity, will eventually observe these two channels.

Our studies of polarized cross sections reveal that the bulk of the total cross section comes from the  $(0, \pm 1)$  helicity state for  $e^+e^- \rightarrow J/\psi + \chi_{c1}$ , and from  $(0, 0)$  and  $(\pm 1, 0)$  helicity states for  $e^+e^- \rightarrow J/\psi + \chi_{c2}$ . It will be interesting for the future Super  $B$  experiments to test these polarization patterns.

On the theoretical side, we have worked out the explicit asymptotic expressions of all the ten NLO helicity amplitudes for the  $e^+e^- \rightarrow J/\psi + \chi_{cJ}$  ( $J = 0, 1, 2$ ) processes. We confirm that helicity selection rule is modified logarithmically at NLO in  $\alpha_s$ . The pattern we recognize in these NLO asymptotic expressions lends further support for the speculation



made in Ref. [18]: The hard exclusive processes involving double-quarkonium at leading twist can only host the single collinear logarithm  $\ln s/m_c^2$  at one-loop, while those beginning with the higher twist contributions are always plagued with double logarithms of form  $\ln^2 s/m_c^2$ .

It is of some theoretical interest to reproduce the asymptotic expressions for the helicity-conserving channels such as  $e^+e^- \rightarrow J/\psi(0) + \chi_{c0,2}(0)$  in the light-cone approach. This should be definitely feasible, which is guaranteed by the leading-twist factorization theorem. Nevertheless, it is much more challenging for the light-cone approach to reproduce, and resum, those process-dependent double logarithms associated with the helicity-suppressed channels.

*Note added.* After the calculation was finished and while we were preparing the draft, a related work appeared in arXiv recently [43], which also investigated the  $\mathcal{O}(\alpha_s)$  correction to the processes  $e^+e^- \rightarrow J/\psi + \chi_{cJ}$  ( $J = 0, 1, 2$ ) within NRQCD factorization approach. Once taking the same input parameters as theirs, and summing up the contributions from all the helicity states, our results agree with Ref. [43] on the numerical sizes of the NLO corrections to the unpolarized cross sections for each  $J = 0, 1, 2$ .

## Acknowledgments

We are grateful to Loretta Robinette for valuable help on proofreading. This research was supported in part by the National Natural Science Foundation of China under Grant No. 10875130, 10935012, by China Postdoctoral Science Foundation, and by the U. S. Department of Energy under Grant No. DE-FG02-93-ER40762.

- 
- [1] G. P. Lepage and S. J. Brodsky, Phys. Rev. D **22**, 2157 (1980).
  - [2] V. L. Chernyak and A. R. Zhitnitsky, Phys. Rept. **112**, 173 (1984).
  - [3] M. Beneke, G. Buchalla, M. Neubert and C. T. Sachrajda, Phys. Rev. Lett. **83**, 1914 (1999) [arXiv:hep-ph/9905312].
  - [4] M. Beneke, G. Buchalla, M. Neubert and C. T. Sachrajda, Nucl. Phys. B **591**, 313 (2000) [arXiv:hep-ph/0006124].
  - [5] K. Abe *et al.* [BELLE Collaboration], Phys. Rev. Lett. **89**, 142001 (2002).
  - [6] B. Aubert *et al.* [BABAR Collaboration], Phys. Rev. D **72**, 031101 (2005) [arXiv:hep-ex/0506062].
  - [7] G. T. Bodwin, E. Braaten and G. P. Lepage, Phys. Rev. D **51**, 1125 (1995) [Erratum-ibid. D **55**, 5853 (1997)] [arXiv:hep-ph/9407339].
  - [8] E. Braaten and J. Lee, Phys. Rev. D **67**, 054007 (2003) [Erratum-ibid. D **72**, 099901 (2005)] [arXiv:hep-ph/0211085].
  - [9] K. Y. Liu, Z. G. He and K. T. Chao, Phys. Lett. B **557**, 45 (2003) [arXiv:hep-ph/0211181].
  - [10] K. Hagiwara, E. Kou and C. F. Qiao, Phys. Lett. B **570**, 39 (2003) [arXiv:hep-ph/0305102].
  - [11] Y. J. Zhang, Y. j. Gao and K. T. Chao, Phys. Rev. Lett. **96**, 092001 (2006) [arXiv:hep-ph/0506076].
  - [12] B. Gong and J. X. Wang, Phys. Rev. D **77**, 054028 (2008) [arXiv:0712.4220 [hep-ph]].
  - [13] J. P. Ma and Z. G. Si, Phys. Rev. D **70**, 074007 (2004) [arXiv:hep-ph/0405111].
  - [14] A. E. Bondar and V. L. Chernyak, Phys. Lett. B **612**, 215 (2005).
  - [15] V. V. Braguta, arXiv:0811.2640 [hep-ph].

- [16] Y. J. Zhang, Y. Q. Ma and K. T. Chao, Phys. Rev. D **78** (2008) 054006 [arXiv:0802.3655 [hep-ph]].
- [17] P. Pakhlov *et al.* [ Belle Collaboration ], Phys. Rev. **D79**, 071101 (2009). [arXiv:0901.2775 [hep-ex]].
- [18] Y. Jia, J. X. Wang and D. Yang, arXiv:1012.6007 [hep-ph].
- [19] M. Jacob and G. C. Wick, Annals Phys. **7**, 404 (1959) [Annals Phys. **281**, 774 (2000)].
- [20] H. E. Haber, arXiv:hep-ph/9405376.
- [21] S. J. Brodsky and G. P. Lepage, Phys. Rev. D **24**, 2848 (1981).
- [22] J. H. Kuhn, J. Kaplan and E. G. O. Safiani, Nucl. Phys. B **157**, 125 (1979).
- [23] G. T. Bodwin and A. Petrelli, Phys. Rev. D **66**, 094011 (2002) [arXiv:hep-ph/0205210].
- [24] J. Kublbeck, M. bohm and A. Denner, Comput. Phys. Commun. **60**, 165 (1990).
- [25] T. Hahn, Comput. Phys. Commun. **140** (2001) 418 [arXiv:hep-ph/0012260].
- [26] R. Mertig, M. Bohm, and A. Denner, Comput. Phys. Commun. **64**, 345 (1991)
- [27] M. Beneke and V. A. Smirnov, Nucl. Phys. B **522**, 321 (1998) [arXiv:hep-ph/9711391].
- [28] G. T. Bodwin, X. Garcia i Tormo and J. Lee, Phys. Rev. Lett. **101**, 102002 (2008) [arXiv:0805.3876 [hep-ph]].
- [29] Z. z. Song and K. T. Chao, Phys. Lett. B **568**, 127 (2003) [arXiv:hep-ph/0206253].
- [30] Z. Z. Song, C. Meng, Y. J. Gao and K. T. Chao, Phys. Rev. D **69**, 054009 (2004) [arXiv:hep-ph/0309105].
- [31] M. Beneke and L. Vernazza, Nucl. Phys. B **811**, 155 (2009) [arXiv:0810.3575 [hep-ph]].
- [32] A. V. Smirnov, JHEP **0810**, 107 (2008). [arXiv:0807.3243 [hep-ph]].
- [33] T. Hahn and M. Perez-Victoria, Comput. Phys. Commun. **118**, 153 (1999).
- [34] Y. Jia and D. Yang, Nucl. Phys. B **814** (2009) 217 [arXiv:0812.1965 [hep-ph]].
- [35] Y. Jia, Phys. Rev. D **76** (2007) 074007 [arXiv:0706.3685 [hep-ph]].
- [36] B. Gong, Y. Jia and J. X. Wang, Phys. Lett. B **670** (2009) 350 [arXiv:0808.1034 [hep-ph]].
- [37] G. P. Lepage and S. J. Brodsky, Phys. Lett. B **87**, 359 (1979).
- [38] A. V. Efremov and A. V. Radyushkin, Phys. Lett. B **94** (1980) 245.
- [39] G. T. Bodwin, J. Lee, C. Yu, Phys. Rev. **D77**, 094018 (2008). [arXiv:0710.0995 [hep-ph]].
- [40] E. J. Eichten and C. Quigg, Phys. Rev. D **52**, 1726 (1995) [arXiv:hep-ph/9503356].
- [41] W. Buchmüller and S.-H. H. Tye, Phys. Rev. D **24**, 132 (1981) [arXiv:hep-ph/9503356].
- [42] K. Abe *et al.* [Belle Collaboration], Phys. Rev. D **70**, 071102 (2004) [arXiv:hep-ex/0407009].
- [43] K. Wang, Y. -Q. Ma, K. -T. Chao, Phys. Rev. **D84**, 034022 (2011). [arXiv:1107.2646 [hep-ph]].

# Erratum: $\mathcal{O}(\alpha_s)$ corrections to $J/\psi + \chi_{cJ}$ production at $B$ factories [JHEP 1110, 141 (2011)]

Hai-Rong Dong<sup>\*,1</sup> Feng Feng<sup>†,2</sup> and Yu Jia<sup>‡1,3</sup>

<sup>1</sup>*Institute of High Energy Physics, Chinese Academy of Sciences, Beijing 100049, China*

<sup>2</sup>*Center for High Energy Physics, Peking University, Beijing 100871, China*

<sup>3</sup>*Theoretical Physics Center for Science Facilities,  
Chinese Academy of Sciences, Beijing 100049, China*

In Ref. [1], we study the  $\mathcal{O}(\alpha_s)$  corrections to  $e^+e^- \rightarrow J/\psi(\psi') + \chi_{cJ}$  ( $J = 0, 1, 2$ ) in NRQCD factorization approach. These next-to-leading order (NLO) perturbative corrections are calculated at the level of helicity amplitude. There are some errors in equations (3.3), (3.4), (4.5), (4.6) and (4.7). Fortunately, these incorrect expressions have not been used in our computer program, therefore all the figures and tables in Ref. [1] need not be modified.

There is one typo in the tree-level NRQCD short-distance coefficient associated with the helicity state  $\gamma^* \rightarrow J/\psi(\pm 1) + \chi_{c2}(0)$ , as given in (3.3c). The corrected coefficients  $c_{\lambda_1, \lambda_2}^J(r)$  ( $J = 0, 1, 2$ ) now read

$$c_{0,0}^0(r) = 1 + 10r - 12r^2 \quad c_{1,0}^0(r) = 9 - 14r, \quad (3.3a)$$

$$c_{0,1}^1(r) = -\sqrt{6}(2 - 7r) \quad c_{1,0}^1(r) = -\sqrt{6}r \quad c_{1,1}^1(r) = -2\sqrt{6}(1 - 3r), \quad (3.3b)$$

$$c_{0,0}^2(r) = \sqrt{2}(1 - 2r - 12r^2) \quad c_{0,1}^2(r) = \sqrt{6}(1 - 5r) \quad c_{1,0}^2(r) = \sqrt{2}(3 - 11r), \\ c_{1,1}^2(r) = 2\sqrt{6}(1 - 3r) \quad c_{1,2}^2(r) = 2\sqrt{3}. \quad (3.3c)$$

Note that  $c_{1,0}^2(r)$  was mistyped as  $\sqrt{2}(11 - 3r)$  in Ref. [1]. To be compatible with the phase convention of the helicity amplitude projector used in Ref. [2], we also include a minus sign for some entries in (3.3). These changes obviously do not affect our numerical predictions for the polarized cross sections.

For the expression that relates the coefficients  $c_{\lambda_1, \lambda_2}^J(r)$  and the leading-order polarized cross section, as given in (3.4), we have missed a factor  $r^{1+|\lambda_1+\lambda_2|}$  in the right side. The correct formula should read

$$\sigma^{(0)}[J/\psi(\lambda_1) + \chi_{cJ}(\lambda_2)] = \frac{32\pi e_c^2 \alpha^2 C_F^2 \alpha_s^2}{3s^2 m_c^6} \left( \frac{|\mathbf{P}|}{\sqrt{s}} \right) R_{J/\psi}^2(0) R_{\chi_{cJ}}'^2(0) r^{1+|\lambda_1+\lambda_2|} |c_{\lambda_1, \lambda_2}^J(r)|^2. \quad (3.4)$$

We also made an error on the overall normalization in the asymptotic expressions of all the ten reduced NLO helicity amplitudes,  $K_{\lambda_1, \lambda_2}^J$  ( $J = 0, 1, 2$ ) in Ref. [1]. All the expressions (except  $K_{1,0}^2$ ) should be multiplied by an overall factor of 4. Since our computer code implemented the correct asymptotic expressions, Figures 2, 3, 4 in Ref. [1] remain intact.

The asymptotic expressions of two reduced NLO helicity amplitudes for  $J/\psi + \chi_{c0}$  should read

$$K_{0,0}^0 \left( r, \frac{\mu^2}{s} \right)_{\text{asym}} = -\frac{1}{3}(4 - \ln 2) \ln r + \frac{\beta_0}{4} \left( \ln \frac{4\mu^2}{s} + \frac{8}{3} \right) \\ - \frac{1}{18}(46 + \pi^2 - 40 \ln 2 + 33 \ln^2 2) + \frac{i\pi}{4} \left( \beta_0 - \frac{16}{3} + \frac{4}{3} \ln 2 \right), \quad (4.5a)$$

$$K_{1,0}^0 \left( r, \frac{\mu^2}{s} \right)_{\text{asym}} = \frac{1}{3} \ln^2 r - \frac{1}{108}(139 - 104 \ln 2) \ln r + \frac{\beta_0}{4} \left( \ln \frac{4\mu^2}{s} + \frac{17}{9} \right) \\ - \frac{1}{54} \left( 161 + \frac{8\pi^2}{3} - \frac{495}{2} \ln 2 + 100 \ln^2 2 \right) + \frac{i\pi}{4} \left( \frac{8}{3} \ln r + \beta_0 - \frac{1}{27}(139 - 104 \ln 2) \right). \quad (4.5b)$$

\* E-mail: donghr@ihep.ac.cn

† E-mail: fengf@ihep.ac.cn

‡ E-mail: jiay@ihep.ac.cn

The asymptotic expressions of the three reduced NLO helicity amplitudes for  $J/\psi + \chi_{c1}$  should read

$$r K_{1,0}^1 \left( r, \frac{\mu^2}{s} \right)_{\text{asym}} = -\frac{1}{12} \left\{ 5 \ln^2 r + (7 - 2 \ln 2) \ln r - 19 + 2\pi^2 + 75 \ln 2 - 21 \ln^2 2 \right. \\ \left. + i\pi(10 \ln r + 7 - 2 \ln 2) \right\}, \quad (4.6a)$$

$$K_{0,1}^1 \left( r, \frac{\mu^2}{s} \right)_{\text{asym}} = \frac{1}{24} \left\{ \frac{25}{2} \ln^2 r - (46 - 99 \ln 2) \ln r + 6\beta_0 \left( \ln \frac{4\mu^2}{s} + \frac{13}{6} \right) \right. \\ \left. - \frac{1}{6}(616 + 74\pi^2 - 1696 \ln 2 + 303 \ln^2 2) + i\pi(25 \ln r + 6\beta_0 - 46 + 99 \ln 2) \right\}, \quad (4.6b)$$

$$K_{1,1}^1 \left( r, \frac{\mu^2}{s} \right)_{\text{asym}} = \frac{1}{24} \left\{ 10 \ln^2 r + 2(1 + 17 \ln 2) \ln r + 6\beta_0 \left( \ln \frac{4\mu^2}{s} + \frac{13}{6} \right) \right. \\ \left. - \frac{1}{3}(266 + 7\pi^2 - 128 \ln 2 + 147 \ln^2 2) + 2i\pi(10 \ln r + 3\beta_0 + 1 + 17 \ln 2) \right\}. \quad (4.6c)$$

The asymptotic expressions of the five reduced NLO helicity amplitudes for  $J/\psi + \chi_{c2}$  should read

$$K_{0,0}^2 \left( r, \frac{\mu^2}{s} \right)_{\text{asym}} = -\frac{1}{3}(4 - \ln 2) \ln r + \frac{\beta_0}{4} \left( \ln \frac{4\mu^2}{s} + \frac{8}{3} \right) \\ - \frac{1}{18}(64 + \pi^2 + 104 \ln 2 + 33 \ln^2 2) + \frac{i\pi}{4} \left( \beta_0 - \frac{10}{3} + \frac{4}{3} \ln 2 \right), \quad (4.7a)$$

$$K_{0,1}^2 \left( r, \frac{\mu^2}{s} \right)_{\text{asym}} = \frac{1}{12} \left\{ \frac{13}{2} \ln^2 r - (22 - 43 \ln 2) \ln r + 3\beta_0 \left( \ln \frac{4\mu^2}{s} + \frac{8}{3} \right) \right. \\ \left. - \frac{1}{6}(284 + 30\pi^2 - 380 \ln 2 + 159 \ln^2 2) + i\pi(13 \ln r + 3\beta_0 - 14 + 43 \ln 2) \right\}, \quad (4.7b)$$

$$K_{1,0}^2 \left( r, \frac{\mu^2}{s} \right)_{\text{asym}} = \frac{1}{6} \left\{ 2 \ln^2 r + \frac{1}{6}(5 + 8 \ln 2) \ln r + \frac{3}{2}\beta_0 \left( \ln \frac{4\mu^2}{s} + \frac{7}{3} \right) \right. \\ \left. - \frac{1}{18}(291 - 8\pi^2 + 171 \ln 2 + 312 \ln^2 2) + i\pi \left( 4 \ln r + \frac{3}{2}\beta_0 + \frac{11}{6} + \frac{4}{3} \ln 2 \right) \right\}, \quad (4.7c)$$

$$K_{1,1}^2 \left( r, \frac{\mu^2}{s} \right)_{\text{asym}} = \frac{1}{24} \left\{ 4 \ln^2 r - (46 - 62 \ln 2) \ln r + 6\beta_0 \left( \ln \frac{4\mu^2}{s} + \frac{13}{6} \right) \right. \\ \left. - \frac{1}{3}(274 + 27\pi^2 - 316 \ln 2 + 9 \ln^2 2) + i\pi(8 \ln r + 6\beta_0 - 46 + 62 \ln 2) \right\}, \quad (4.7d)$$

$$K_{1,2}^2 \left( r, \frac{\mu^2}{s} \right)_{\text{asym}} = -\frac{1}{4} \left\{ 2 \ln^2 r + \frac{2}{3}(1 + 13 \ln 2) \ln r - \beta_0 \left( \ln \frac{4\mu^2}{s} + \frac{5}{3} \right) \right. \\ \left. + \frac{1}{9}(-7\pi^2 + 140 - 104 \ln 2 + 237 \ln^2 2) - i\pi \left( \beta_0 + 3 - \frac{26}{3} \ln 2 \right) \right\}. \quad (4.7e)$$

Note that the overall factor in (4.7c) was mistakenly typed as  $-\frac{1}{88}$  in Ref. [1]. In the current formulas, the renormalization scale  $\mu$  enters the  $K_{\lambda_1, \lambda_2}^J$  functions in the form of  $\frac{\beta_0}{4} \ln \frac{4\mu^2}{s}$  unanimously, which stems from the renormalization group invariance of each NLO polarized cross section for  $e^+e^- \rightarrow J/\psi + \chi_{c0,1,2}$ .

- [2] J. Xu, H. -R. Dong, F. Feng, Y. -J. Gao and Y. Jia, arXiv:1212.3591 [hep-ph].